THE JOURNAL OF PHYSICAL CHEMISTRY B

Article

pubs.acs.org/JPCB

Real-Time Observation of Polymer Network Formation by Liquid- and Solid-State NMR Revealing Multistage Reaction Kinetics

Michael Kovermann,[†] Kay Saalwächter,[‡] and Walter Chassé*[,‡]

[†]Institut für Physik—Biophysik, Martin-Luther-Universität Halle-Wittenberg, Betty-Heimann-Str. 7, D-06120 Halle, Germany

[‡]Institut für Physik—NMR, Martin-Luther-Universität Halle-Wittenberg, Betty-Heimann-Str. 7, D-06120 Halle, Germany

ABSTRACT: The reaction rate for the end-cross-linking process of vinyl-terminated poly(dimethylsiloxane) by a cross-linker with four Si−H functionalities in the presence of solvent was studied by ^{1}H liquid-state NMR in dependence of the reaction temperature. The properties of the resulting polymer networks, i.e., the gel-point and the formation of the elastically effective network, were monitored *in situ* during the reaction by single-evolution-time ^{1}H double-quantum (SET-DQ) low-field NMR. It was found that the cross-linking kinetics shows no uniform reaction order for the conversions of the functional groups before the topological gelation threshold of the polymer network. The two NMR methods are combined to investigate the formation of the elastically effective network in dependence of the conversion of the functional groups of the precursor polymers and the cross-linker. The high chemical and time resolution of the experiments enabled an in-depth analysis of the reaction kinetics, allowing us to conclude on a multistage model for PDMS network formation by hydrosilylation-based end-linking in the presence of solvent. We found that the nonuniform network formation kinetics originates from a dependence of the apparent reaction rate on the number of the Si−H groups of the cross-linker that have already reacted during the progress of the reaction. The fastest overall reaction rate is observed in a range until each cross-linker has reacted once on average, and a uniform apparent overall reaction order of unity with respect to cross-linker concentration is only found at a later stage, when multiply reacted cross-linker molecules with similar reactivity dominate.

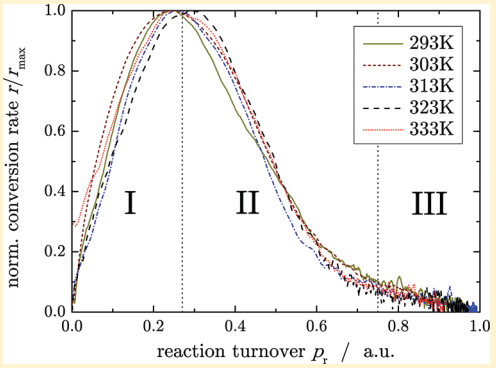

INTRODUCTION

Poly(dimethylsiloxanes) (PDMS) are prominent examples for the versatility of current polymer network materials. The resistance to light degradation, chemical attack, and high temperatures, and of course the extraordinary mechanical properties, render PDMS-based materials applicable as sealant, adhesive, and anticorrosion materials, especially for biomedical uses.

PDMS networks are typically formed by covalent cross-linking of randomly or end-functionalized polysiloxanes and multifunctional cross-linkers with complementary reactive groups. These networks are often used as so-called model networks in studies of rubber elasticity and structure−property relations due to their well-defined cross-link chemistry. A very efficient and frequently used approach is the Pt-catalyzed hydrosilylation[1] of vinyl-terminated poly(dimethylsiloxane) by cross-linkers with silane functionalities. The permanent cross-links are established by addition of the silane-hydrogen to the carbon−carbon double bond, forming an ethylene connection between polymer and cross-linker. The reaction is commonly described by the Chalk−Harrod[2] or the modified Chalk−Harrod[3] mechanism.

The hydrosilylation reaction has been the subject of intense investigations. Many studies show a strong dependence of the reaction kinetics on the molecular structure and type of the catalyst[4−6] and the initial concentration of the functional groups and their stoichiometry.[7] Usually the kinetics are monitored by observation of the chemical conversion of specific functional groups with spectroscopic methods, e.g., FTIR[8] and NMR.[5,6,9] Especially for the reaction order, different results are reported.[5,6,10]

In this work, we present an in depth study of the cross-linking and network formation kinetics of the end-linking process of vinyl-terminated PDMS by a four-functional cross-linker in the presence of solvent. An equal-molar formulation of the polymer and cross-linker is investigated at different reaction temperatures to obtain information about the relevant activation energy. The conversion of the terminal vinyl-groups and the Si−H groups is monitored by high-resolution ^{1}H liquid-state NMR. The high time resolution of the performed experiments allows a detailed discussion of the conversion rates and the reaction order of the hydrosilylation.

The formation of the elastically effective network is investigated by ^{1}H double-quantum (DQ) NMR. This approach uses the fact that the NMR response changes during the cross-link process. In melts, and especially in the presence

Received: March 22, 2012
Revised: May 31, 2012
Published: May 31, 2012

of solvent, polymers behave like liquids unless their molecular weight is not far above the entanglement molecular weight M_e. Inter- and intra-monomer dipolar couplings between ^{1}H spin-pairs are completely averaged out by fast segmental fluctuations of the polymer chain. Restrictions, i.e., chemical cross-links and entanglements, constrain the polymer motions. They become anisotropic, and weak residual dipolar couplings persist. Thereby, the anisotropy of the motions is directly proportional to the nature and severity of topological restrictions in which the polymer chains are involved. In this way, the detectable residual dipolar couplings correlate with the physical and chemical cross-link density of polymer networks. In this study, a single-point detection technique for the DQ intensity[11] is used to investigate the formation kinetics of the networks, since the recording of full DQ build-up curves leads to an insufficient time resolution. Combining the observations of the kinetics in terms of chemical conversion and in terms of elastic network-chain formation as a function of temperature, we are able to draw conclusions on the rate-limiting steps in the end-linking reaction by hydrosilylation.

EXPERIMENTAL SECTION

Sample Preparation. In this study, a commercially available (ABCR) vinyldimethylsiloxy-terminated poly(dimethylsiloxane), ePDMS21, and a nominally 4-functional cross-linker, tetrakis(dimethylsiloxy)silane, were used. The prepolymer was characterized by gel permeation chromatography (GPC) using a polystyrene standard. The determined average molecular weight was $M_n \approx 4.8$ kg/mol with a polydispersity of about 2. The average functionality of the cross-linker, turning out to be 3.6 by the ratio of the methyl and Si−H groups, and the precise ratio of the vinyl-functionalized terminal monomers to the dimethylsiloxy monomers were both determined by ^{1}H liquid-state NMR. The catalyst, *cis*-dichlorobis(diethylsulfide)platinum(II),[12,13] was dissolved in 98% toluene.

For the investigation of the cross-link kinetics by ^{1}H liquid-state NMR and ^{1}H low-field DQ NMR, all samples were prepared following the same protocol. The un-cross-linked polymer was dissolved in 200 wt % deuterated toluene with respect to the used amount of polymer and mixed by a shaker at 1200 rpm for about 5 min. This corresponds to a semidilute solution with a polymer concentration about 10 times higher than the overlap concentration ($c^* \approx 0.035$ wt %) and significantly reduced viscosity, facilitating the fast mixing of the reactants. The 3.6-functional cross-linker was added to this solution in a stoichiometric ratio and shaken again. The necessary amount of cross-linker was calculated with regards to the results of the sample characterization by liquid-state NMR. From this parent solution, 700 μL was filled into the NMR sample tubes. For liquid-state and solid-state NMR experiments, 5 and 10 mm tubes, respectively, were used. The sample tubes were placed for about 5 min in the preheated spectrometer for temperature equilibration. After adding 2.5 μL of the catalyst solution, the tubes were sealed carefully with Teflon strips and the measurements were immediately started.

^{1}H Liquid-State NMR Experiments. All ^{1}H liquid-state NMR experiments were performed on a Bruker Avance III 600 MHz spectrometer, using a deuterium lock to avoid and compensate field drifts during the long-time experiments. The cross-link reaction was followed by a pseudo-2D experiment composed of consecutive 1D ^{1}H free induction decay (FID) experiments. The time resolution of the liquid-state NMR experiments was adjusted with respect to the cross-linking temperature T_{cr} by changing the number of scans used for the acquisition of a single FID. The time increments were in the range of 11−60 s for reaction temperatures of 343−293 K, respectively. The recorded 1D experiments of a cross-link reaction were separately processed for reasons of data quality.

^{1}H Solid-State NMR Experiments. The ^{1}H DQ solid-state NMR experiments were carried out on a Bruker minispec *mq*20 spectrometer operating at a ^{1}H resonance frequency of 20 MHz with a 90° pulse length of 2.2 μs and a dead time of 13 μs. The experiments and the analysis of the measured raw data were performed following the previously published procedures.[14,15]

In this study, we used ^{1}H DQ low field NMR to determine the residual dipolar couplings. Several publications have shown that ^{1}H DQ NMR is a robust and versatile tool for the quantitative investigation of the structure of polymer networks.[14,16−18] The main advantage of this method is the acquisition of two time-dependent sets of data, the double-quantum build-up and the reference decay curve, by different phase cycling schemes in the pulse sequence with a variable evolution time τ_{DQ} for the excitation and reconversion of multiquantum coherences. The intensity of the double-quantum signal $I_{DQ}(\tau_{DQ})$ contains the $(4n + 2)$-quantum coherences and comprises the structural information of the network. The intensity of the reference signal $I_{ref}(\tau_{DQ})$ contains the dipolar modulated longitudinal magnetization and all $4n$-quantum coherences. Additionally, isotropic mobile fractions of the polymer networks, i.e., network defects, contribute to I_{ref}. The defect fraction has a rather slow relaxation as compared to elastically active network components,[19] which allows a precise identification and subtraction of the contribution to I_{ref}. With the two measured signal intensity curves, it is possible to remove the relaxation effects by a point-by-point division of I_{DQ} by the sum of both signals.

$$I_{nDQ} = \frac{I_{DQ}}{I_{DQ} + I_{ref} - \text{defects}} \quad (1)$$

After a proper subtraction of the defect contribution, the normalized double-quantum build-up I_{nDQ} (eq 1) is dominated by pure dipolar interactions that are only related to the network structure. The information about the residual dipolar couplings and their distributions are obtained by fitting functions or numerical inversion procedures. In this study, we used the recently introduced improved Tikhonov regularization procedure to determine the average residual dipolar coupling constant D_{res} of the investigated samples.[15]

The recording of a complete DQ build-up curve takes about 20−60 min. Thus, the method is not suited for the investigation of fast cross-linking processes. To overcome this limitation to the observation of very slow reactions, we use a single point detection to investigate the network formation.[11] This approach is based on the notion that the DQ intensity exclusively arises from contributions of the elastically effective network. The DQ intensity is recorded at a fixed single evolution time (SET) during the whole cross-linking reaction.

In order to test the validity and reliability of this approach, a cross-link reaction at 313 K was investigated by SET-DQ NMR and completely recorded DQ build-up curves (full-DQ). At this temperature, the network formation is just slow enough to be followed by a full-DQ experiment with minimum recycle delay. The results of the full-DQ measurements were evaluated according to the procedure which was explained above. The

dx.doi.org/10.1021/jp302745a | J. Phys. Chem. B 2012, 116, 7566−7574

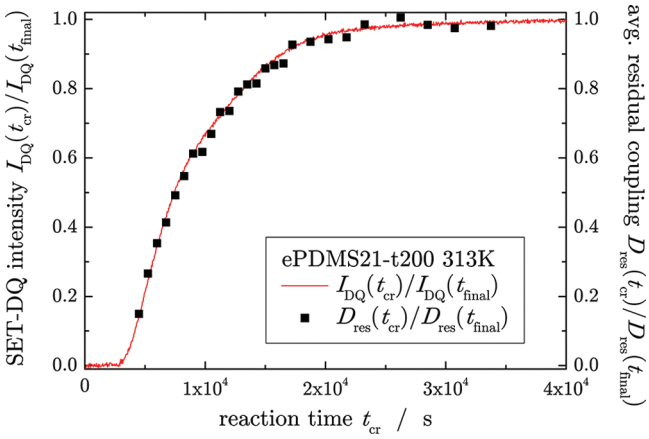

Figure 1. Normalized SET-DQ intensity nI_{DQ} and scaled average residual dipolar coupling constant nD_{res} in dependence of the reaction time of a cross-linking reaction performed at 313 K.

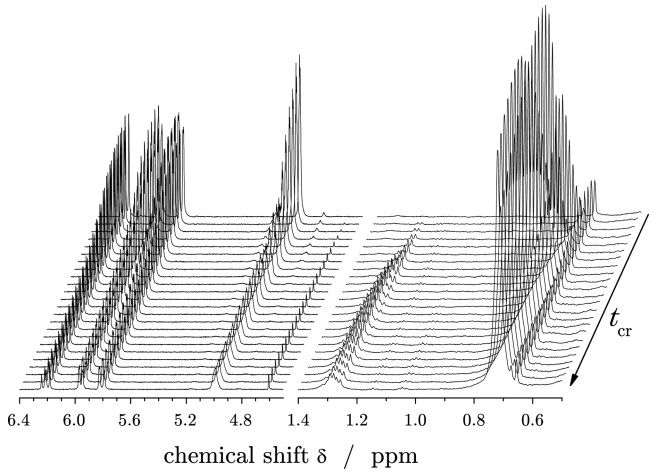

Figure 2. ^{1}H liquid-state NMR spectra acquired during the first 20 min during a cross-link reaction at 333 K showing the functional groups, vinyl (6.3...5.7 ppm) and silane (~5 ppm), and the α and β addition products of the reaction in the aliphatic region at 1.35...1.2 and 0.8...0.6 ppm, respectively. The small signal at 4.6 ppm, rising further at longer raction times, is an unknown side product.

results of both methods, SET-DQ intensities and residual dipolar couplings, respectively, are shown in Figure 1 and are both normalized by the results for the fully cured samples. The very good agreement of the dependence on the reaction time t_{cr} confirms that both methods are equally suitable for the investigation of gelation kinetics. The clear advantage of the SET-DQ approach is the much higher time resolution, which allows for the investigation of the sol−gel transition. In contrast to the full-DQ measurements, no information about the sol fraction and the coupling constant distribution is obtained during the cross-link reaction. Below, we demonstrate that all reactions, independent of the reaction temperature, show a comparable progress of the DQ intensity with the reaction turnover obtained from liquid-state NMR. Therefore, it can be assumed that distributions and sol-fractions obtained at a certain reaction turnover by full-DQ experiments during slow reaction also reflect these in fast reactions at the same reaction turnover.

Finally, we point out again that the SET-DQ intensity represents no quantitative estimate for the residual dipolar coupling strength, since it is measured in arbitrary units and is not normalized. The presented dependency of the SET-DQ intensity on the cross-link time t_{cr} just yields information about the relative change of the effective cross-link density.

RESULTS AND DISCUSSION

In the present work, the end-linking of vinyl-terminated PDMS in the presence of solvent reducing the viscosity and enabling better mixing at the initial stages was investigated in dependence on the reaction temperature T_{cr}. First, we will show the results of the high-resolution liquid-state NMR measurements of the reaction kinetics. The reaction-time-dependent formation of the resulting elastically effective network is discussed in the second part. Finally, we investigate the coupling constant distributions and the defect fractions of the obtained PDMS networks and demonstrate the universality of the network formation process.

Reaction Kinetics of Semidilute PDMS Solutions. In order to study the cross-linking kinetics and the reaction rate constants in the semidilute PDMS systems, the conversions of the functional groups of the vinyl-terminated precursor polymers and the (nominally) four-functional cross-linker were estimated by liquid-state NMR. Figure 2 shows ^{1}H NMR spectra obtained for a semidilute PDMS/cross-linker solution of 33 wt % polymer at different reaction times t_{cr}. The signals of the vinyl-group protons (6.3...5.7 ppm) and the silane proton (~5 ppm) of the cross-linker are well-defined, and the different chemical shift allows an independent evaluation of the conversion of the functional groups. It is important to stress that the liquid-state NMR observations remain quantitative up to the gelation threshold of the systems. While network-like components (characterized by finite residual dipolar couplings) may be broadened beyond detection in the high-resolution spectra, isotropically mobile dangling structures remain visible even above gelation. This is why vinyl group signals (which are always attached to a sol or a dangling chain) are visible throughout the whole reaction, and the good agreement of the vinyl signal with the total cross-linker signal (see below) shows that indeed also the multiply reacted cross-linker remains quantitatively visible up to high conversions.

The integrated signals of the vinyl and silane groups directly reflect their concentration in the semidilute system, and have the expected ratio of 3:1 according to the different number of protons belonging to the functional groups. This ratio was observed to be approximately constant for all investigated reactions. Therefore, the impact of potential competitive secondary reactions, i.e., the formation of Si−OH groups by oxidation or hydrolysis of the silane-group with oxygen or water, respectively, on the conversion of the silane groups is minor or even negligible. For vinyl groups, no secondary reactions are reported in the literature for the temperature range used in this work. Therefore, the conversion of the terminal vinyl groups is taken to represent the overall conversion p_r for the study of the kinetics, ensuring that only primary network-forming reactions are investigated.

The signals at 1.35...1.2 ppm and 0.8...0.6 ppm in Figure 2 belong to the two different kinds of cross-links which are formed during the hydrosilylation reaction. The Markovnikov process (α addition) leads to a 1,1-ethylene cross-link, and the anti-Markovnikov process (β addition), to an 1,2-ethylene cross-link. The analysis of the recorded kinetics shows that 14−18% of the cross-links were formed by the α addition, which corresponds to values observed for hydrosilylation reactions in

dx.doi.org/10.1021/jp302745a | J. Phys. Chem. B 2012, 116, 7566−7574

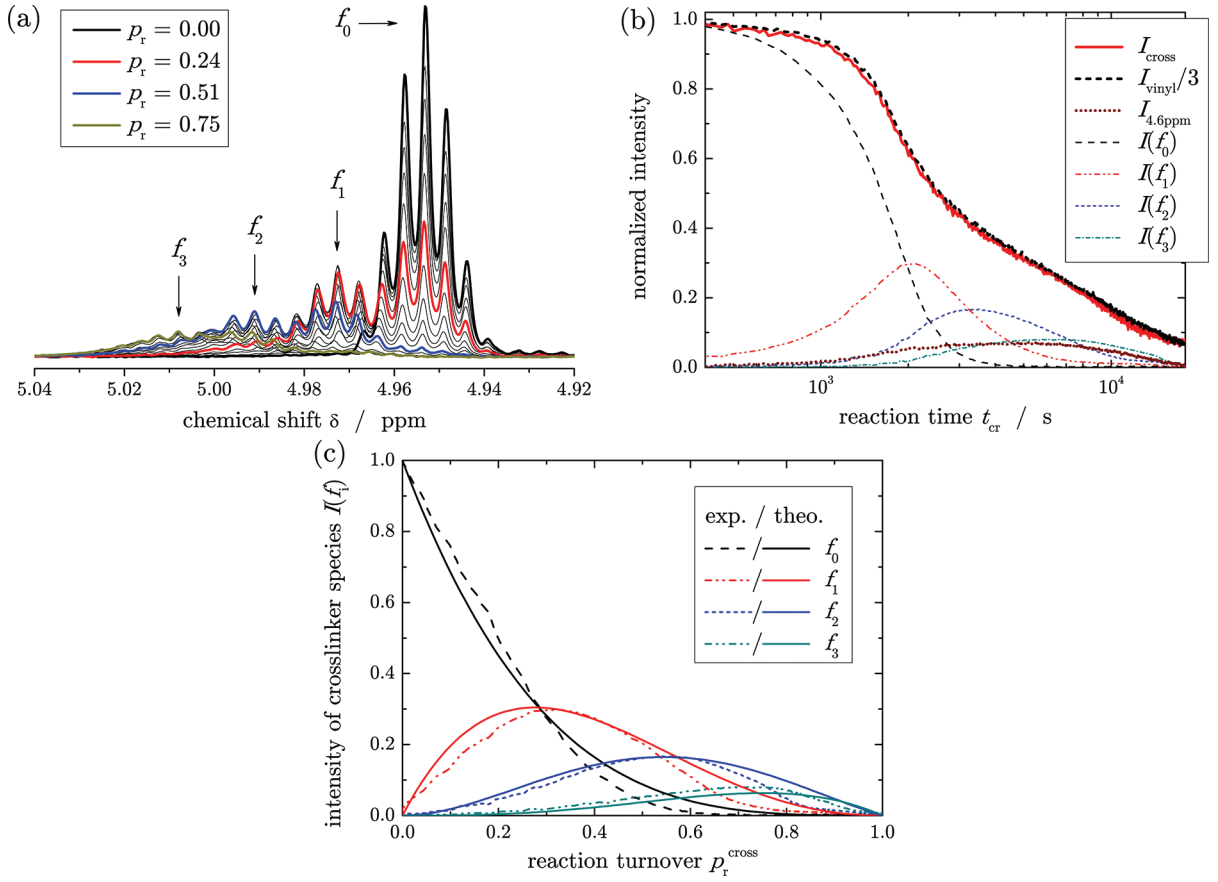

Figure 3. (a) Evolution of the cross-linker ^{1}H signal during a cross-linking reaction at 313 K. f_i indicates the central spectral line of the i-fold reacted cross-linker. (b) Time-dependent intensities of the cross-linker, vinyl group, and side product (4.6 ppm) signal, as well as the fractions f_i of I_{cross} (thin lines), normalized with respect to $I_{cross}(t_{cr} = 0)$. (c) Comparison of the relative signals of the different cross-linker species determined during the cross-link reaction, along with theoretical predictions based on Bernoulli statistics in dependence on the reaction turnover of the cross-linker p_r^{cross}.

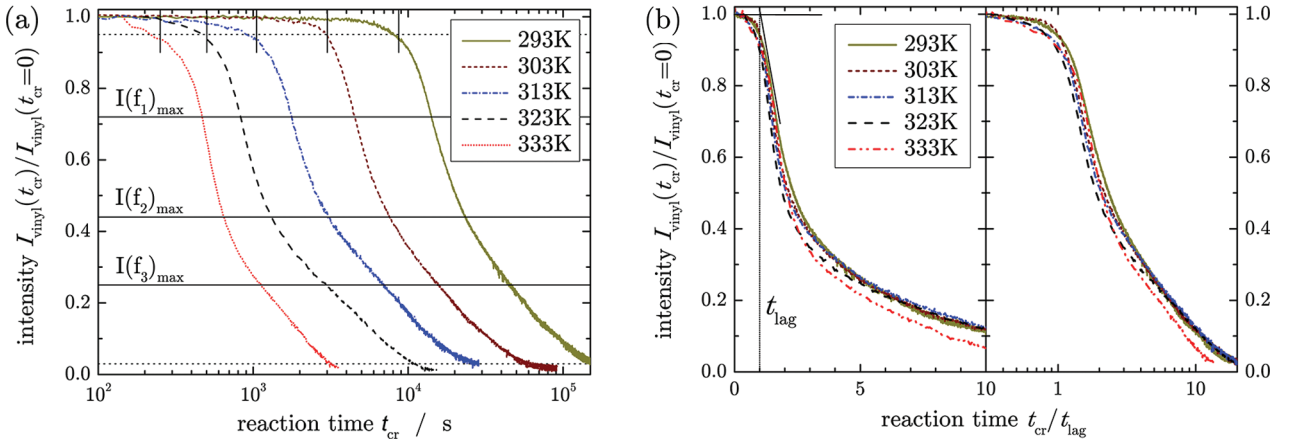

Figure 4. (a) Evolution of the integrated vinyl intensity determined by ^{1}H liquid-state NMR during the end-linking process in the PDMS/toluene system in dependence on reaction time t_{cr}. The intensities are normalized to the intensity at $t_{cr} = 0$, and lag times t_{lag} are indicated by vertical bars. (b) Vinyl intensity I_{vinyl} vs linear (left) and logarithmic (right) reaction time t_{cr}, scaled with respect to t_{lag}, as determined from the intercept of the steepest tangent with $y = 1$ in the linear representation, as indicated by the lines in the left panel in part b.

the literature.[20] The fraction of formed β products slightly increases at higher cross-link temperatures. Additionally, a signal of rather low intensity, attributed to a side product, is observed at 4.6 ppm in Figure 2.

Figure 3a shows a detailed view of the cross-linker Si−^{1}H resonances recorded during a cross-link reaction at 313 K at different reaction times. The signal of the remaining Si−H groups of an i-times reacted cross-linker molecule is obviously shifted in dependence of the number of reacted functional sites. Each of the subsignals is the septed expected for a single Si−H J-coupled to 6 methyl protons. We attribute this shift to changes in the overall conformational dynamics when different numbers of chains are attached.

dx.doi.org/10.1021/jp302745a | J. Phys. Chem. B 2012, 116, 7566−7574

The equivalent dependence of the vinyl- and Si−H intensity on the reaction time shown in Figure 3b demonstrates that both are consumed in equal amounts during the cross-link reaction, and the observed dependencies yield no clear information about the origin of the additional signal at 4.6 ppm, which reaches about 10% with respect to the initial cross-linker signal and vanishes again by the end of the overall reaction. We currently have no explanation for this significant side product, but point out that the corresponding signal is not "missing" in the overall signal balance; the signal of all vinyl groups is at any time identical to 3 times the total cross-linker signal, and the aliphatic signals of the formed cross-links are at any time the exact intensity complement.

The progress of the reacted functional sites of the cross-linker is shown in Figure 3b and c, where in the latter it is plotted as a function of the reaction turnover of the cross-linker p_r^{cross}. The data on the relative amounts were obtained by integration of the central lines of the respective septets marked in Figure 3a, which does not lead to significant errors related to the overlap of the multiplets. In Figure 3c, this data is compared with theoretical predictions based on simple Bernoulli statistics, assuming statistically independent reaction probabilities for the four sites of the cross-linker, and equating these probabilities p_r with the reaction turnover. For example, the fraction f_1 is given by $4(1 - p_r)^3 p_r$. For the theory lines in Figure 3c, it was taken into account that the signals for the fractions f_i correspond to $(4 - i)$ protons. The higher f_i are thus underrepresented (f_4 is not detectable, as it has no Si−H anymore). Finally, it was further considered that the average functionality of the cross-linker is actually 3.6, which means the data can be thought of as being represented by 60 and 40% 4- and 3-functional linker molecules, respectively. With all these details considered, we observe very satisfactory agreement of the experimental data and the predictions, confirming a well-behaved cross-linking reaction.

Figure 4a shows the integrated vinyl group intensities I_{vinyl} of the ^{1}H NMR spectra measured *in situ* during the end-cross-linking process in dependence of the reaction time t_{cr} for different temperatures T_{cr}. The results were normalized with respect to their initial intensity $I_{vinyl}(t_{cr} = 0)$ and plotted on a logarithmic time scale to amplify the different stages of the reaction. Three main periods can be identified in Figure 4a for the conversion of the vinyl groups. This corresponds to results reported in the literature for platinum complex-catalyzed hydrosilylation reactions.[21,22] In the first part of the reaction, the induction period, the active species of the catalyst is formed. This is followed by the reaction period, in which the majority of the vinyl-groups is consumed in a fast exothermic reaction. In the final postcuring period, the reaction is very slow due to the low concentration of the reactants and steric hindrances. The different reaction periods can also be distinguished by the horizontal solid lines in Figure 4a, which represent the turnovers for which each of the stepwise reacted cross-linker species is maximal.

The induction period is characterized by a rather slow conversion of the functional groups. Such an induction period was also observed in previous kinetic studies[21] but never analyzed in more detail due to the lack of experimental accuracy (mainly time resolution). The length of the induction period, the lag time t_{lag}, can be identified by a steepest-tangent construction; see Figure 4b. The so-obtained lag times are used as a scaling factor for the reaction time in the same figure. The comparable dependence of I_{vinyl} on the scaled reaction time clearly demonstrates the uniform progress of the cross-link reaction at all investigated temperatures. Obviously, the whole reaction kinetics follow more or less the same temperature dependence, which is at the earliest stage reflected in t_{lag}. The rather small deviations can be attributed to minor inaccuracies during the preparation of the semidilute PDMS/cross-linker solution. The evaluation of the lag time t_{lag} in dependence on the reaction temperature in an Arrhenius plot yields an activation energy of about $E_a \approx 74$ kJ/mol for the rate-limiting step of the investigated reaction.

The conversion profiles of the vinyl-groups in the reaction period show a complex dependence on the reaction time t_{cr}. The data in Figure 4a and b already indicate that the overall reaction kinetics cannot be described by a simple single exponential first-order or power-law-type second-order rate equation. In order to obtain more information about the conversion rate constants, the reaction kinetics were explicitly evaluated according to a first-order reaction as well to a second-order reaction. For both, no uniform dependence of the conversion rate on the reaction time and the turnover was observed over the entire reaction period. Especially between 5 and 75% conversion of the vinyl groups, the measured kinetic profiles clearly deviate from the typical behavior of first- and second-order reaction kinetics. An analysis in terms of reaction rate constants was thus not possible.

Figure 5 shows the conversion rate r of the vinyl groups in dependence on the fraction of vinyl groups consumed during

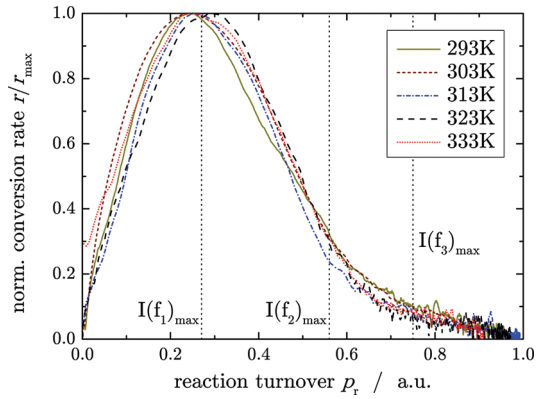

Figure 5. Normalized conversion rate r vs reaction turnover p_r of the terminal vinyl-groups. Conversion rates were determined by a direct time derivative of the integrated vinyl intensities shown in Figure 4. The vertical dotted lines indicate the dominant i-times reacted cross-linker species.

the cross-linking process, the reaction turnover p_r. The conversion rate is directly obtained by the derivative of the integrated vinyl intensity with respect to the reaction time, $r = dI_{vinyl}(t_{cr})/dt_{cr}$, and normalized by the respective maximum rate r_{max}. Independent on the reaction temperature T_{cr}, the investigated cross-link reactions all have the same dependence of the normalized conversion rate on the reaction turnover. At the start of the cross-linking process, the conversion rate rapidly increases and reaches its maximum rate r_{max} at reaction turnovers of about 25%. This feature is particularly indicative of a complex process without a well-defined reaction order. In the later stages of the reaction, the conversion rate continuously decreases. At first, a very rapid decay of the rate r is observed beyond the maximum. This decay distinctly decelerates at roughly 60% reaction turnover. For reaction turnovers above

dx.doi.org/10.1021/jp302745a | J. Phys. Chem. B 2012, 116, 7566−7574

75%, only a slow near-linear decrease of the conversion rate is observed.

Discussion of the Complex Reaction Kinetics. We assume that the observed behavior of the conversion rate r can solely be attributed to the number of *residual functional sites* of the cross-linker molecules in the polymer/solvent system. For times larger than t_{lag}, the dependence of the intensity (=concentration) of the completely nonreacted cross-linker $I(f_0)$ on the reaction time t_{cr} shown in Figure 3b can indeed be described by a first-order reaction, i.e., by a singly exponential decay. The observation of a first-order reaction is expected from the published mechanism,[2,3] where the initial stage involves a homolytic cleavage of the Si−H bond of the cross-linker and binding of both fragments to the metal center. A dependence on the vinyl concentration is then not expected, and the observation of a (pseudo-) first-order reaction with respect to the vinyl concentration is a mere consequence of the stoichiometry. Our observations thus allow for conclusions on the rate-limiting step.

Along with the decay of $I(f_0)$, the cross-linker species with less residual functional sites f_1, f_2, and f_3 populate in a stepwise manner, as also shown in Figure 3b. Initially, the reaction involves the addition of unreacted cross-linker molecules to single vinyl functionalities. At around 25% reaction turnover, all cross-linker molecules have reacted once on average, and this indeed coincides well with the observed maximum intensity of the once-reacted species of the cross-linker, $I(f_1)_{max}$. The latter is observed at approximately 27% reaction turnover, which can be attributed to the estimated average functionality of 3.6 of the used cross-linker. The ongoing reaction of the once-reacted cross-linker after the rate maximum (where f_0 is almost completely gone) follows again a first-order decay but with a lower apparent rate. The same behavior is observed for the intensities of the cross-linker species with two or one residual functional sites, $I(f_2)$ and $I(f_3)$, respectively. Despite the observed first-order kinetics of the different cross-linker species $I(f_i)$, this behavior is not reflected in the *overall* conversion of cross-linker, and also not in the vinyl group concentration of the polymer chains, as shown in Figure 4a. This can be rationalized by the coexistence of the different cross-linker species, which therefore appear to feature different apparent reaction rates. The overall conversion of the functional groups as observed in the total NMR intensity only yields the average conversion rate for all species.

The recorded complex overall reaction kinetics of the vinyl groups obviously arises from the different reaction rates associated with the cross-linker species that are mostly populated in different stages of the reaction, as indicated by the vertical dotted lines in Figure 5. This is why the conversion of the functional groups can be described only partially by first-order reactions with different reaction rates. Especially at low reaction turnovers ($p_r < 0.5$), the distinctly different populations of the different cross-linker species preclude a description of the overall reaction kinetics by a simple singly exponential first-order rate equation. In particular, the unreacted (f_0) and the once-reacted cross-linker (f_1) appear to have a larger reactivity. The decaying apparent reactivity may simply be related to the decreasing number of close-by reactive groups; in other words, the Si−H concentration is locally increased in an as-yet unreacted four-functional cross-linker. The increasingly bulky nature of the substituents of the Si atom of the cross-linker unit that binds to the catalytic center may also play an indirect role.

As is apparent from Figure 3b, the induction period is mainly characterized by an increase of the conversion rate of the unreacted cross-linker f_0. The maximum rate is observed when 30−50% of it are consumed. The origin of this autocatalytic feature remains unclear at present; we can only state that it cannot be explained by an increased local concentration of Si−H groups around a given metal center, since it is observed for the unreacted and not for the once-reacted cross-linker. A viable hypothesis would be that the catalyst in its initial state must go through one catalytic cycle, thus changing its structure and becoming more reactive. From the consideration of the activation energies below, this first cycle must, however, have the same rate-limiting step as the ensuing cycles.

At higher reaction turnovers ($p_r > 0.75$), the number of the residual functionalities of the cross-linker molecules decreases significantly below two on average. The f_1 species then loses more and more of its dominant influence on the conversion rate, while f_2 and f_3 appear to have more similar reactivities. Only in this range, the apparent reaction order can indeed be estimated from a double-logarithmic representation of the *total* conversion rate r versus the concentration of vinyl groups, $1 - p_r$. Linear fits to the data in the region between 75 and 95% reaction turnover yield slopes between 0.95 and 1.09. The slope in such a representation directly reflects the reaction order of the investigated process, which thus follows approximately a uniform first-order reaction kinetics. In this range, the same dependence is observed for the conversion of the Si−H groups. As mentioned, we attribute the observation of a pseudo-first-order reaction with respect to the vinyl concentration to be due to the fixed stoichiometry

At this point, we propose a three-stage model to describe the kinetics of an end-linking process with multifunctional cross-linkers in the presence of solvent. In the first stage, the increasing conversion rate is determined by an autocatalytic process involving mainly a reaction with the unreacted cross-linker f_0, and the increasing conversion of this and the once-reacted cross-linker species. When the conversion rate of the f_0 species has reached its maximum, its ensuing reaction is well described by first-order kinetics. In the second state beyond the maximum overall conversion rate, the apparently more reactive zero- and once-reacted cross-linkers diminish, and multiply reacted and apparently less reactive cross-linker species become dominant, but still no uniform overall reaction order can be observed. This is followed by the third stage, during which the conversion of multiply reacted cross-linker species dominates and follows a first-order reaction kinetics, as does the overall conversion of vinyl groups.

Activation Energy of the Cross-Link Reaction. The investigated hydrosilylation reaction in the presence of solvent exhibits a complex progress of the conversion of the functional groups with the reaction time t_{cr}, as shown above. This of course prevents an evaluation of the reaction kinetics with respect to global conversion rates. Therefore, the conversion rates at certain reaction turnovers p_r were used to estimate the activation energy of the reaction. Figure 6 shows the conversion rates at several reaction turnovers as an Arrhenius plot. For all selected reaction turnovers, a linear dependence of $\ln(r)$ on the inverse reaction temperature T_{cr}^{-1} is observed. The figure shows again the large difference in the conversion rates at different points of the cross-link reaction. A global linear fit to the data yields an activation energy of $E_a = 73.7 \pm 2.2$ kJ/mol. The latter is within the error equal to the activation energy obtained above by evaluation of the length of the induction period, and

dx.doi.org/10.1021/jp302745a | J. Phys. Chem. B 2012, 116, 7566−7574

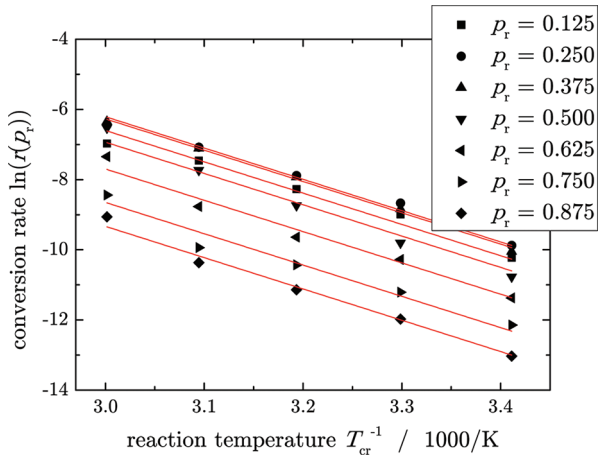

Figure 6. Dependence of the vinyl group conversion rates r at different reaction turnovers on the reaction temperature T_{cr}^{-1}. The rates were obtained by direct time-derivation of the vinyl intensities.

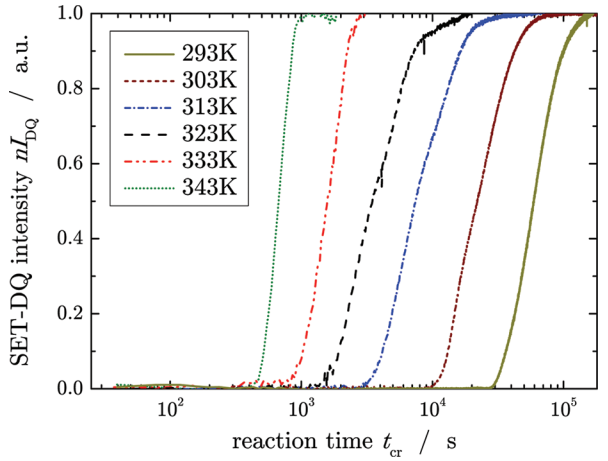

Figure 7. Evolution of normalized DQ intensities nI_{DQ} at a fixed DQ-evolution time, τ_{DQ} = 1.317 ms, for different cross-link temperatures T_{cr} in dependence on reaction time t_{cr}.

corresponds to values given in the literature.[10] The global fit shows a remarkably good agreement with the data for all investigated reaction turnovers. This confirms that the reaction is in *every* stage rate-limited by the same reaction step that is of course part of a complex multistep mechanism.

The simplest a priori assumption explaining the uniform activation energy and the complexity of the cross-linking reaction would actually be to assume diffusion control. Then, the nonuniform reaction rates beyond the maximum could be related to the changing large-scale mobility of the cross-linking components, and the activation energy would characterize the rate-limiting basic process of molecular transport through the semidilute solution. This option must, however, be ruled out on the basis of the high value of the activation energy. It is distinctly higher than the activation energy E_a^D for the diffusion coefficient of PDMS in toluene, that is reported to be around 14 kJ/mol.[23] We have performed additional pulsed-gradient NMR diffusion experiments on the PDMS and toluene components of our semidilute solutions, and confirmed that E_a^D in our system is almost equal for the two components and of similar magnitude as the literature value, further confirming a possible description on the basis of a common effective friction coefficient. This leaves us with the above-discussed combination of an autocatalytic initial stage and decreasing reactivity for multiply reacted cross-linker species as the origin of the overall rate profile shown in Figure 5. Since we observe well-defined first-order kinetics for the concentration of the Si−H groups of the unreacted cross-linker after the induction time, we conclude that the rate-limiting step of the reaction with the given activation energy involves the homolytic cleavage of the Si−H bond upon binding to the catalytic metal center.

Formation of the Elastically Effective Network. The evolution of the elastically effective polymer network was investigated by low-field ^{1}H single-evolution-time double-quantum (SET-DQ) NMR. The DQ evolution time τ_{DQ} used for the measurements during the cross-linking process was obtained from a complete DQ build-up curve recorded for a fully cured ePDMS21 sample. The time at which the normalized DQ intensity reaches 50% of its maximum was used as DQ evolution time τ_{DQ}. The latter was kept constant for all measurements.

Figure 7 shows the results of the real-time SET-DQ NMR experiments during the cross-link reaction in dependence on the reaction time t_{cr} for a series of different reaction temperatures T_{cr}. The results were normalized with respect to the DQ intensities of the fully cured gels and plotted on a logarithmic time scale to clarify the strong temperature dependence of the investigated gelation process. The reaction times at which the final extent of the cross-link reaction is observed range from 15 min at T_{cr} = 343 K up to 40 h at T_{cr} = 293 K.

The recorded formation kinetics can be separated into three main stages. In the first part of the reaction, the *pregel phase*, the measured DQ intensity is equal to zero. Orientation dependent dipole−dipole couplings are averaged out completely by the fast isotropic motions of the short and unentangled polymers. In the *formation period*, the NMR response of the polymers is partially solid-like. The formation of a network due to the chemical linkage of the polymer chains by permanent covalent bonds leads to restrictions of the polymer mobility. The latter becomes anisotropic, and some dipolar couplings persist. The strength of these observable residual dipolar couplings is directly proportional to the number of restrictions which the polymer chains are subject to. The contribution of entanglements and/or packing effects to the DQ intensity I_{DQ} can be assumed as negligible, since the cross-linking is performed under conditions of dilution by solvent, and the molecular weight of the used precursor polymers is far below M_e. Therefore, the recorded DQ intensity $I_{DQ}(t_{cr})$ directly reflects the evolution of the cross-link density of the elastically effective network. Finally, a very slow *postcuring process* is observed, which is characterized by small changes of I_{DQ} at very long reaction times, until no further notable increase is detected. This stage corresponds to the last stage observed for the vinyl-group conversion by the ^{1}H liquid-state NMR experiments.

The build-up of the DQ-intensity in the *formation period* in Figure 7 was analyzed by an exponential rate equation, $I_{DQ} \sim e^{-k_{gel}t_{cr}}$. The evaluation of the so-obtained gelation rates, k_{gel}, in dependence on the reaction temperature in an Arrhenius plot yields an activation energy of E_a = 74.3 ± 3.6 kJ/mol. This is again in very good agreement with the activation energies obtained from the investigation of the lag times and the conversion rates of the terminal vinyl groups. The equal temperature dependence of the conversion rate r and the gelation rate k_{gel} demonstrates that indeed the DQ-intensity directly reflects the cross-link density of polymer networks.

dx.doi.org/10.1021/jp302745a | J. Phys. Chem. B 2012, 116, 7566−7574

Estimation of the Gel-Point. The transition between the liquid- and solid-like NMR response of the polymer chains is equivalent to the sol−gel transition and is characterized as an apparent gelation time. For a detailed investigation of the gelation process, and especially the gel point, the results obtained by the two NMR methods are combined. Figure 8

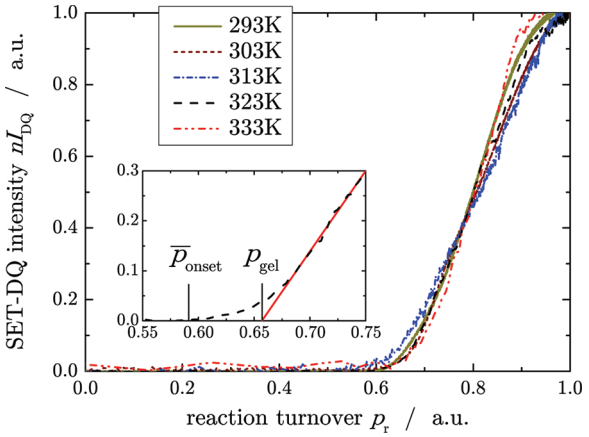

Figure 8. Formation of the elastically effective network in dependence on the reaction turnover. The inset shows an enlargement of the sol−gel transition region for a sample cross-linked at T_{cr} = 323 K. p_{gel} indicates the gel point obtained by linear extrapolation (dotted line).

shows the evolution of the SET-DQ intensity as a function of the reaction turnover p_r. Only above a certain reaction turnover of around 65%, a noticeable DQ intensity is observed, which exhibits a continuous crossover into a near-linear dependence on the reaction turnover. This behavior, which is clearly illustrated by the inset in Figure 8, is observed for all investigated cross-link temperatures. We assume that the continuous sol−gel transition can be attributed to the formation of small network-like domains or microgels in the solution which raise detectable residual dipolar couplings. Therefore, the topological gelation threshold is not straightforwardly reflected by the first observation of a recognizable DQ intensity at $\overline{p}_{onset}$, as loosely defined in ref 11. For a more precise estimation, the observed and expected linear dependence of the DQ intensity on the reaction turnover is used to determine the gel-point, p_{gel}, by linear extrapolation. The evaluation of the temperature dependence of the corresponding gelation times t_{gel} in an Arrhenius representation yields an activation energy of again E_a = 72.1 ± 3.3 kJ/mol. This is in very good agreement with all activation energies determined during this study and confirms again that the reaction proceeds in every stage with the same local reaction mechanism.

Network Characterization. The network structure of the fully cured samples was investigated by low-field ^{1}H DQ NMR. The average residual dipolar coupling constant, D_{res}, and its variance, σ, were determined by numerical analysis (regularization) of the normalized DQ build-up curves. The experiments were performed on dry network samples after complete and careful evaporation of the solvent. The defect fraction, $\omega_{def,sw}$, of the networks was determined by ^{1}H DQ NMR experiments on equilibrium swollen samples.[24]

The results of the network characterization (see Table 1) show a very good agreement for the determined properties of the networks, which were cured during the high- and low-field NMR studies of the reaction kinetics. The observed deviations are within the experimental error of the DQ experiment or can

Table 1. Results of Network Characterization by ^{1}H Low-Field DQ Experiments on Fully Cured Networks Previously Investigated by High-Field (hf) and Low-Field (lf) NMR Experiments after Evaporation of the Toluene-d_8[a]

	$D_{res}/2\pi$ (kHz)		σ/D_{res}		$\omega_{def,sw}$	
T_{cr} (K)	hf	lf	hf	lf	hf	lf
293	0.164	0.165	0.31	0.23	0.18	0.18
303	0.159	0.173	0.28	0.26	0.18	0.20
313	0.161	0.161	0.31	0.26	0.22	0.20
323	0.160	0.166	0.31	0.28	0.21	0.16
333	0.163	0.159	0.25	0.31	0.16	0.20

[a] D_{res} and σ were obtained by regularization of I_{nDQ}. $\omega_{def,sw}$ was determined in an equilibrium swollen sample.

be attributed to slight inaccuracies in the preparation of the samples. Overall, this demonstrates that networks with nearby equal properties are formed during the cross-link reaction independent on the cross-link temperature.

CONCLUSIONS

In this study, the reaction kinetics of the hydrosilylation and the formation of the elastically effective network were investigated during the end-cross-linking process in a semidilute PDMS system. For the first time, we could identify deviations from a simple exponential time dependence of the conversion on the reaction time, as reflected in the concentration of the vinyl groups at the PDMS chain ends and the four Si−H units of the cross-linker molecule. The precise estimation of the conversion of the terminal functional groups of the polymers by real-time ^{1}H liquid-state NMR and the high time resolution of the experiments enabled a direct investigation of the conversion rates during the entire progress of the reaction and thus an in-depth analysis of the reaction kinetics.

The results show a complex dependence of the overall conversion rate on the reaction turnover, revealing an induction period and a maximum rate at around 25% conversion (stage I), and an apparently nonuniform reaction order also beyond the conversion rate maximum (stage II). The constantly changing number of residual reaction sites of the cross-linker molecules leads to different dominating species throughout the reaction, and the reactivity (apparent conversion rate constant) of these species is found to decrease with an increasing number of already reacted Si−H sites. Only at higher reaction turnovers (stage III), an apparent first-order reaction kinetics can be observed for the overall conversion of either the total amount of Si−H or vinyl groups, presumably because multiply reacted cross-linker molecules show similar apparent reactivity.

The consistent observation of the same activation energy derived from the different observables taken at different stages and from different experiments based on molecular conversion, or chain dynamics revealing the topological network formation, confirms that the network formation is rate-limited by the same local mechanism. Diffusion control and flow activation as a possible origin can be ruled out on the basis of the high value of the activation energy of about 74 kJ/mol. Since the conversion of the Si−H groups of the unreacted cross-linker molecules at the early stage after the induction period also follows a first-order kinetics, we assign the rate-limiting step to the homolytic cleavage of the Si−H groups upon binding to the catalytic metal center. The observation of a pseudo-first-order reaction

dx.doi.org/10.1021/jp302745a | J. Phys. Chem. B 2012, 116, 7566−7574

kinetics for the vinyl group conversion is merely a consequence of the stoichiometry.

AUTHOR INFORMATION

Corresponding Author

*E-mail: walter.chasse@physik.uni-halle.de.

Notes

The authors declare no competing financial interest.

ACKNOWLEDGMENTS

The authors are indebted to Frank Lange and Alexey Krushelnitzky for performing the pulsed-gradient diffusion experiments and for valuable discussions. We further thank Prof. Jochen Balbach for extensive spectrometer time.

REFERENCES

(1) Speier, J. L.; Webster, J. A.; Barnes, G. H. *J. Am. Chem. Soc.* **1957**, *79*, 974−979.
(2) Chalk, A. J.; Harrod, J. F. *J. Am. Chem. Soc.* **1965**, *87*, 16−21.
(3) Chung, L. W.; Wu, Y.-D.; Trost, B. M.; Ball, Z. T. *J. Am. Chem. Soc.* **2003**, *125*, 11578−11582.
(4) Dez-González, S.; Nolan, S. P. *Acc. Chem. Res.* **2008**, *41*, 349−358.
(5) Caseri, W.; Pregosin, P. *J. Organomet. Chem.* **1988**, *356*, 259−269.
(6) Coqueret, X.; Wegner, G. *Organometallics* **1991**, *10*, 3139−3145.
(7) Esteves, A.; Brokken-Zijp, J.; Laven, J.; Huinink, H.; Reuvers, N.; Van, M.; de With, G. *Polymer* **2009**, *50*, 3955−3966.
(8) Hammouch, S. O.; Beinert, G. J.; Herz, J. E. *Polymer* **1996**, *37*, 3353−3360.
(9) Bonnet, J.; Bounor-Legaré, V.; Boisson, F.; Mélis, F.; Cassagnau, P. *J. Polym. Sci., Part A: Polym. Chem.* **2011**, *49*, 2899−2907.
(10) Antíc, V. V.; Antíc, M. P.; Govedarica, M. N.; Dvorníc, P. R. *J. Polym. Sci., Part A: Polym. Chem.* **2007**, *45*, 2246−2258.
(11) Saalwächter, K.; Gottlieb, M.; Liu, R.; Oppermann, W. *Macromolecules* **2007**, *40*, 1555−1561.
(12) Roulet, R.; Barbey, C. *Helv. Chim. Acta* **1973**, *56*, 2179−2186.
(13) Horn, G. W.; Kumar, R.; Maverick, A. W.; Fronczek, F. R.; Watkins, S. F. *Acta Crystallogr., Sect. C* **1990**, *46*, 135−137.
(14) Saalwächter, K. *Prog. Nucl. Magn. Reson. Spectrosc.* **2007**, *51*, 1−35.
(15) Chassé, W.; Valentín, J. L.; Genesky, G. D.; Cohen, C.; Saalwächter, K. *J. Chem. Phys.* **2011**, *134*, 044907.
(16) Saalwächter, K.; Herrero, B.; López-Manchado, M. A. *Macromolecules* **2005**, *38*, 9650−9660.
(17) Graf, R.; Heuer, A.; Spiess, H. W. *Phys. Rev. Lett.* **1998**, *80*, 5738−5741.
(18) Valentín, J. L.; Carretero-González, J.; Mora-Barrantes, I.; Chassé, W.; Saalwächter, K. *Macromolecules* **2008**, *41*, 4717−4729.
(19) McLoughlin, K.; Szeto, C.; Duncan, T. M.; Cohen, C. *Macromolecules* **1996**, *29*, 5475−5483.
(20) Mukbaniani, O.; Titvinidze, G.; Tatrishvili, T.; Mukbaniani, N.; Brostow, W.; Pietkiewicz, D. *J. Appl. Polym. Sci.* **2007**, *104*, 1176−1183.
(21) Stein, J.; Lewis, L. N.; Smith, K. A.; Lettko, K. X. *J. Inorg. Organomet. Polym.* **1991**, *1*, 325−334.
(22) Stein, J.; Lewis, L. N.; Gao, Y.; Scott, R. A. *J. Am. Chem. Soc.* **1999**, *121*, 3693−3703.
(23) Rauch, J. Ph.D. thesis, Universität Bayreuth, 2006.
(24) Chassé, W.; Lang, M.; Sommer, J.-U.; Saalwächter, K. *Macromolecules* **2012**, *45*, 899−912.